Materials Advances

ROYAL SOCIETY OF CHEMISTRY

PAPER

View Article Online
View Journal | View Issue

Cite this: *Mater. Adv.*, 2023, 4, 1671

High mechanically enhanced and degradable polybenzoxazine/polyhexahydrotriazine IPN aerogels by atmospheric drying†

Yi Xu, *[ab] Xinyue Sun,[ab] Keqi Zhu,[ab] Shumin Xu,[ab] Changhui Liu,[ab] Shenghua Xiong[ab] and Chao Li*[c]

Received 15th November 2022,
Accepted 27th February 2023

DOI: 10.1039/d2ma01035f

rsc.li/materials-advances

Oily wastewater and oil spills pose a threat to the environment and human health, and absorbing these harmful organics through porous aerogel materials is an efficient method for oil/water separation. Herein, we design degradable, hydrophobic, and mechanical 4,4′-methylenedianiline polybenzoxazine/silicone-based polyhexahydrotriazine aerogels (BOZ/Si-PHT) for efficient oil/water separation. The BOZ/Si-PHT interpenetrating network (IPN) aerogels were successfully prepared by sequential polymerization, followed by atmospheric drying without any additional post-processing. The as-prepared BOZ/Si-PHT aerogels exhibit prosperous hydrophobicity (a water contact angle of 121.5°) and good mechanical properties (a compressive strength of 449.6 kPa). Meanwhile, the BOZ/Si-PHT aerogels possess good absorption capacity of oils or organic solvents ranging from 4.6 to 16.3 times their own weights. More importantly, the BOZ/Si-PHT aerogels show rapid degradation after use. This work provides simple, environmentally friendly and sustainable materials for oil/water separation and the rationally designed hydrophobic BOZ/Si-PHT aerogels display enormous potential for practical applications dealing with oily wastewater and oil spills.

1 Introduction

In recent years, water pollution has caused serious environmental and ecological problems, due to frequent oil spills.[1–3] So, treatment of oily wastewater has become one of the world's problems in dealing with environmental pollution.[4] To overcome this problem, physical methods,[5] biological methods[6] and chemical methods have been employed for wastewater treatment.[7,8] Among these methods, physical absorption has the advantages of low cost and high efficiency, making it more attractive for oil spill cleanup.[9–11] Silica aerogels have been by far the most widely used commercial aerogels, known for their high porosity and high absorption capacity, making them hopeful alternatives for oil/water separation applications.[12–15] Adsorption capacity of oil/water separation can reach 12.5 g g^{-1} and 8.7 g g^{-1} for silica aerogels modified with TMCS and MTMS, respectively.[12] Excellent adsorption capacity of 8.7–15.4 g g^{-1} has been obtained for ternary flexible silica aerogels modified with dimethyldiethoxysilane (DEDMS), methyltriethoxysilane (MTES) or tetraethoxysilane (TEOS).[16] MTMS/TEOS co-precursor silica aerogels have an absorption capability of as high as 6.48–12 g g^{-1}.[17] Methyltrimethoxysilane (MTMS) derived spherical silica aerogels synthesized *via* a water in-oil emulsion method have been reported, which have an absorption capability as high as 5–11 times their own weight.[18] Despite enormous potential of silica aerogels, these materials have notable limitations for commercial applications due to their poor mechanical properties caused by the fragile skeletal frame linkage. Besides this, supercritical drying or freezedrying processes of silica aerogels also lead to increasing cost and safety risks, and the non-degradability of silica aerogels also produces waste that pollutes the environment. Based on these, improving the mechanical properties, lowering production costs, and ameliorating the degradability of silica aerogels are of great significance for expanding their applications.

To improve the mechanical properties of silica aerogels, polymers are introduced into silica aerogels to solve their brittleness problems. Polyacrylamide,[19,20] polystyrene,[21] polyimide,[22] and epoxy[23] have been reported to improve the mechanical properties of silica aerogels. The elastic deformation of a polyether-based silica aerogel was increased up to 15%, while that of silica aerogels typically varied between 3% and 5%.[21] It has been reported that

[a] College of Civil Aviation Safety Engineering, Civil Aviation Flight University of China, Guanghan, 618307, China. E-mail: xuyi99@cafuc.edu.cn
[b] Civil Aircraft Fire Science and Safety Engineering Key Laboratory of Sichuan Province, Civil Aviation Flight University of China, Guanghan, 618307, China
[c] Chengdu BOE Optoelectronics Technology Co., Ltd, Chengdu, 611731, China. E-mail: lichao_scu@qq.com

† Electronic supplementary information (ESI) available. See DOI: https://doi.org/10.1039/d2ma01035f

amine-modified silica aerogels encapsulated in polyurea exhibit good mechanical properties with up to 77% ultimate failure strain.[24] Silica aerogel–epoxy nanocomposites exhibited significant improvements in tensile strength (62%) and toughness (126%).[23] A silica–polyimide nanocomposite with 28 wt% silica shows 1.4 times higher compressive young's modulus and three times higher stress than those of the pure polyimide aerogel.[25] In order to enhance interactions between polymers and silica aerogels, silica aerogels with functional groups should be first prepared, such as the introduction of ethenyl or amino groups, making the preparation process of composite aerogels redundant. Furthermore, a more dangerous preparation process such as supercritical CO_2 drying is also used in the drying process.

An interpenetrating network (IPN) can induce synergistic enhancement of two types of polymers, because of the simple preparation process. Monomers could be immersed into sol or gel, and then be polymerized to form post-gels. It should be pointed out that gelation and polymerization processes must be orthogonal; namely, the corresponding reagents should not react with one another. Since the aerogel preparation process usually requires a solvent exchange step, the main problem of aerogels is leaching of the polymer from the pores. It is reported that polymethylmethacrylate (PMMA) is completely lost during solvent exchange processing.[26] Interestingly, polyvinylpyridine (PVP) did not leak out from the silica gel due to hydrogen bonding between polymer chains.[27] This report provides a solution, in that the introduction of a polymer having hydrogen bonding with a silica aerogel can effectively improve the entanglement degree of two blending systems. Polybenzoxazine/polyhexahydrotriazine IPNs were successfully prepared by a sequential formation of both networks free of competitive reactions, and exhibit high mechanical and degradable properties.[28] Inspired by this method, it is feasible to prepare polybenzoxazine/silica-containing polyhexahydrotriazine IPN aerogels with high mechanical properties.

In this work, polybenzoxazine/silica-based polyhexahydrotriazine (BOZ/Si-PHT) aerogels with degradability and good mechanical properties are fabricated through sequential cross-linking reactions. The design of BOZ/Si-PHT aerogels is mainly based on the following aspects: (i) rich hydrogen bond donors (*i.e.*, N and OH) from polybenzoxazines could form intermolecular hydrogen bonds with N or O in polyhexahydrotriazine, which could increase the degree of network interpenetration between polymer chains and endow aerogels with good mechanical properties, (ii) the simple atmospheric drying process could be realized because of repulsive interactions between methyl groups,[29] and (iii) the degradable structure of hexahydrotriazine networks formed from PHT could be an amazing property for environmental protection. As a result, the BOZ/Si-PHT aerogels are successfully prepared by atmospheric drying, exhibiting good cyclic compressive mechanical properties (a compressive strength of 449.6 kPa). It is confirmed that the BOZ/Si-PHT aerogels with robust porous structures are a prosperous oil/water separation material with high adsorption capacity (4.6–16.3 g g^{-1}) for various oils and organic solvents, showing their potential to be an ideal decontamination material for applications in environmental protection.

2 Experimental section

2.1 Materials and chemicals

Bis(4-(2*H*-benzo[*e*][1,3]oxazin-3(4*H*)-yl)phenyl)methane (BOZ) was purchased from Chengdu Coryes Polymer Technology Co. 1,3-Bis(3-aminopropyl) tetramethyldisiloxane (98.0%, BATDMS) was purchased from Hangzhou Silong Material Technology Co., Ltd (China). No. 3 aviation kerosene (99.0%) was bought from Jinan Jingyu Chemical Co., Ltd (China). Hydrochloric acid (37%), formalin (37 wt% formaldehyde, FA, in water), *N*-methylpyrrolidone (99%, NMP), dichloromethane (99.8%, CH_2Cl_2), dimethylformamide (99.5%, DMF), acetonitrile (99.8%), ethylacetate (99.0%), tetrahydrofuran (99.9%, THF), toluene (99.8%), chloroform (99.0%, CCl_4), *n*-pentane (99.8%), and Sudan IV ($\geq$98.0%) were obtained from Shanghai Aladdin Chemicals Co. Ltd (China). Deionized water was obtained from our laboratory.

2.2 Preparation of BOZ/Si-PHT aerogels

1 ml of formaldehyde solution (37 wt%) and 1 g of BATDMS and BOZ with different mass (0.1, 0.3, and 0.5 g) were dissolved in ampoules containing 8 mL of NMP, respectively. The obtained solutions were placed in an oven with a stepwise curing program at 50 °C, 4 h, and 180 °C, 6 h. After this, the wet gels were replaced by solvent twice with acetonitrile and *n*-pentane, respectively, with a 24 hour interval between each time. The wet gels were dried at 50 °C, 2 h and 120 °C, 4 h under atmospheric pressure, and the corresponding aerogels were abbreviated as BOZ/Si-PHT-0.1, BOZ/Si-PHT-0.3, and BOZ/Si-PHT-0.5, respectively. The schematic diagram of the preparation process of BOZ/Si-PHT aerogels is shown in Fig. 1(A). From the digital photograph of Fig. 1(B), BOZ/Si-PHT aerogels can be placed stably on the dog's tail grass, which means that the aerogels are very light.

2.3 Characterization

Fourier transform infrared (FT-IR) spectra were obtained using a Nicolet Magna 560 spectrometer with a resolution of 4 cm^{-1} and a scanning mode of 32 times. The morphologies of polymer bulks were observed using a Hitachi s-4800 field emission-scanning electron microscope. The samples were fractured in liquid nitrogen, and then, the fractured surfaces were sputtered with gold and observed at an accelerating voltage of 15 kV. XPS was applied to analyze the chemical composition of the aerogel surface using an Axis Ultra spectrometer (Kratos Analytical, Manchester, UK) with X-radiation l Kα ($h\nu$ = 1486.6 eV). The samples were quantified using the Casa XPS software. Contact angle measurements were carried out using a DSA-30 contact angle system (Kruss, Germany) at room temperature. Ultrapure water was used as the test liquid. Compressive testing was performed using a compressive tester (UTM-5105X, Shenzhen SUNS technology Co., Ltd) equipped with two flat-surface compression stages and a 100 N load cell. Samples under testing were in cylindrical shape with a diameter of 10 mm and a height of 10 mm and were compressed to 20% strain at a given strain rate of 5 mm min^{-1}. Compressive tests were repeated 30 times on samples to study the loading–unloading behaviors.

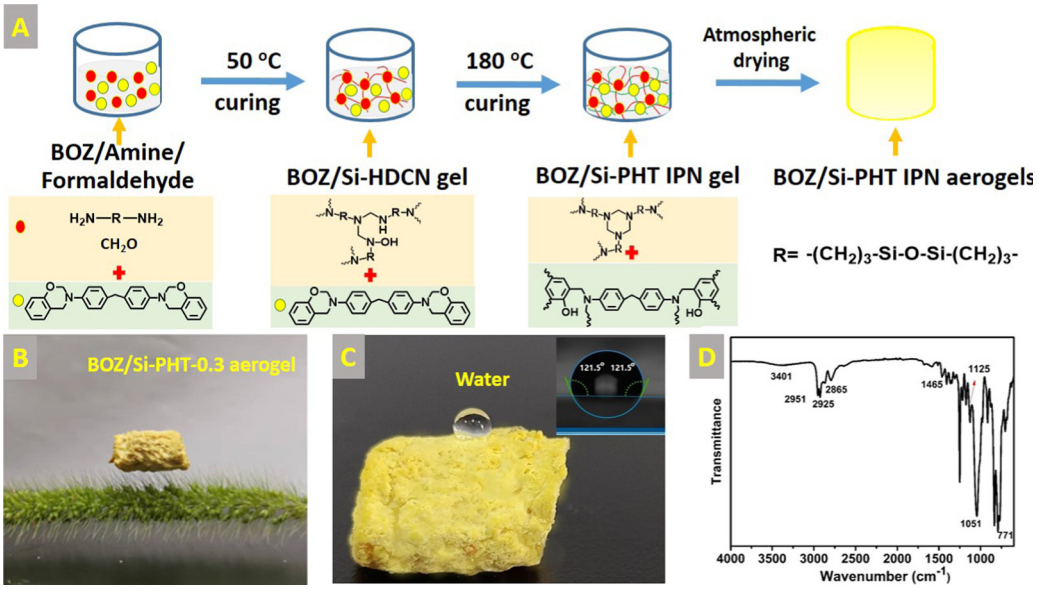

Fig. 1 (A) Schematic diagram of the preparation process of BOZ/Si-PHT IPN aerogels. (B) Digital photographs of the BOZ/Si-PHT-0.3 IPN aerogel. (C) The state of the water droplet on the surface of the BOZ/Si-PHT-0.3 aerogel and the water contact angle (WCA) of the BOZ/Si-PHT-0.3 aerogel. (D) FT-IR spectra of the BOZ/Si-PHT-0.3 aerogel.

3 Results and discussion

3.1 Structural analysis of the BOZ/Si-PHT IPN aerogels

The successful synthesis of BOZ/Si-PHT IPN aerogels was confirmed by FTIR spectroscopy and XPS. Fig. 1D presents the FT-IR spectra of the BOZ/Si-PHT-0.3 IPN aerogel. The characteristic peaks at 2951 cm^{-1} and 1465 cm^{-1} correspond to the symmetric and the asymmetric stretching vibrations of methyl groups, respectively. The absorption bands at 2925 cm^{-1} and 2865 cm^{-1} were assigned to the asymmetric and symmetric stretching vibrations of methylene groups, respectively. The absorption peak at 1051 cm^{-1} corresponds to the stretching vibration of Si–O. The absorption peaks at 1125 cm^{-1} and 771 cm^{-1} correspond to C–N, proving triazine rings formed in BOZ/Si-PHT. Besides, the characteristic peak at 3401 cm^{-1} corresponds to the ring-opening polymerization of oxazine rings. In addition, the XPS survey spectra of BOZ/Si-PHT-0.3 are shown in Fig. S1 (ESI†). BOZ/Si-PHT-0.3 shows the presence of silica in addition to the presence of carbon, nitrogen and oxygen elements. The carbon, oxygen, nitrogen and silica elements show binding energy signals at 286, 400, 533 and 102 eV, respectively. The peak separations of C 1s, O 1s, and N 1s are presented in Fig. 2(A–C) and Table S1 (ESI†), in which these binding energy signals are observed. The peaks observed at 284.8 eV, 285.5 eV and 286.3 eV correspond to the presence of C–H, C–C/C–H, and C–N/C–O groups, respectively.[30,31]

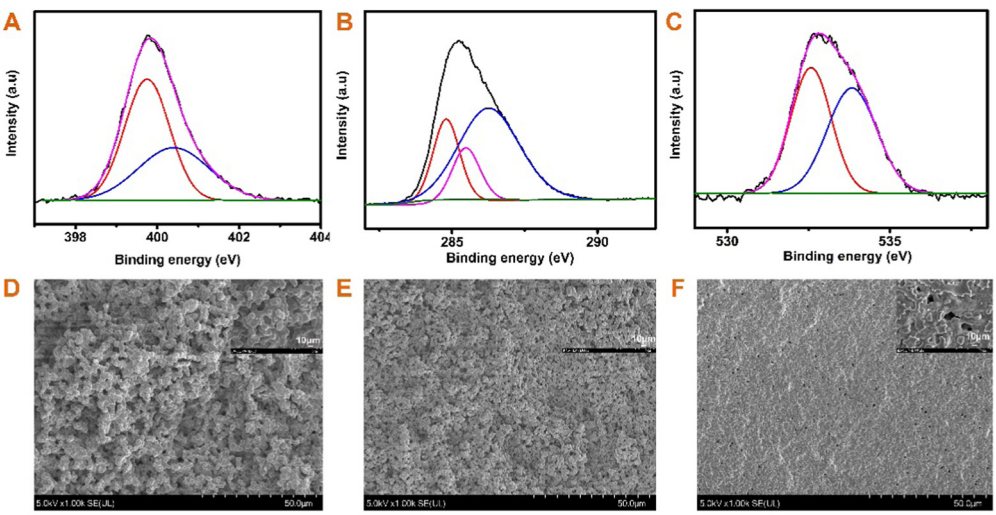

Fig. 2 (A) N 1s XPS of the BOZ/Si-PHT-0.3 aerogel. (B) C 1s XPS of the BOZ/Si-PHT-0.3 aerogel. (C) O 1s XPS of the BOZ/Si-PHT-0.3 aerogel. (D–F) SEM images of the BOZ/Si-PHT-0.1, BOZ/Si-PHT-0.3, and BOZ/Si-PHT-0.5 aerogels, respectively.

The peaks at 399.8 eV and 533.8 eV were assigned to Ar–N and Ar–O from polybenzoxazine, respectively. Meanwhile, the peak at 532.6 eV corresponds to C–N from polyhexahydrotriazine. The results obtained from both XPS and FTIR analyses show the successful formation of polybenzoxazine and silicon-containing polyhexahydrotriazine structures.

The morphologies of bulk BOZ/Si-PHT aerogels were studied by FESEM and are shown in Fig. 2(D–F). With the increasing BOZ content, the particle size of the BOZ/Si-PHT systems becomes smaller, the images of the fracture surface exhibit network structures composed of spherical particulates with sizes of ~12 μm and ~8 μm for BOZ/Si-PHT-0.1 and BOZ/Si-PHT-0.3, respectively, and the particles look as if they have coalesced. Between the spheres, interconnected channels or pores ranging from a few microns to tens of microns are formed. It is thought that the cross-linking of benzoxazine and hexahydrotriazine structures strengthens the skeleton of the polymer gel to withstand capillary pressure. When the BOZ content continues to increase, the pore size of BOZ/Si-PHT-0.5 further decreases. It is speculated that the polybenzoxazine resin covers some pores, resulting in a decrease in pores.

As can be seen from Fig. 3(A, C and E), when the BOZ/Si-PHT aerogels are compressed to 20.0% of their original sizes, they can quickly return to their original sizes after the external force is removed. It is found that with the increase of the BOZ content, the compressive stress of BOZ/Si-PHT-0.5 increases to 449.6 kPa (Table S2, ESI†). After 30 cycles of compression experiments, the heights of BOZ/Si-PHT-0.1, BOZ/Si-PHT-0.3, and BOZ/Si-PHT-0.5 aerogels are 97.6%, 97.5%, and 97.4% of their original heights without external forces, respectively, as shown in Fig. 3(B, D and F). These results prove that due to rigid aromatic structures of polybenzoxazines, the BOZ/Si-PHT aerogels exhibit excellent mechanical behaviors during compression and recovery experiments.

Oil–water separation of functional aerogels has attracted much attention due to their unique porous structures. Here, the wettability of the prepared BOZ/Si-PHT aerogels was systematically investigated to reveal their potential for oil/water separation applications. As shown in Fig. 1C, a water droplet can maintain its spherical shape on the BOZ/Si-PHT-0.3 aerogel surface, showing hydrophobic properties. Owing to the rough surface structure and the hydrophobicity of BOZ/Si-PHT-0.3, the WCA value of the BOZ/Si-PHT-0.3 aerogel was about 121.5°, demonstrating intrinsic good hydrophobicity even without any external surface treatment. To simulate the removal of oils from water, carbon tetrachloride dyed by Sudan IV was dropped at the bottom of water, as shown (Movies S1–S3, ESI†). When the BOZ/Si-PHT aerogels were added into water and brought into contact with CCl_4 droplets, they absorb CCl_4 from water within 1 s, showing excellent organic solvent absorption from water. BOZ/Si-PHT aerogels could also absorb jet fuel dyed by Sudan IV above water quickly (Fig. 4A–C). 15 mg of BOZ/Si-PHT aerogels absorb 10 mL of jet fuel and the water becomes clear within 1 min, 1.5 min, and 3 min for the BOZ/Si-PHT-0.1, BOZ/Si-PHT-0.3, and BOZ/Si-PHT-0.5 aerogels, respectively. Although fast adsorption behaviors from water were assigned to the hydrophobic structures of BOZ/Si-PHT aerogels, the adsorption capacities of BOZ/Si-PHT aerogels decrease obviously when the content of BOZ increases to 0.5 g. The possible reason is that the holes of aerogels are occupied by polybenzoxazines and the specific surface areas decrease. Fig. 4(D and E) illustrate the adsorption capacities of BOZ/Si-PHT aerogels for various oils and organic solvents, including jet fuel, *n*-pentane, *N*-methylpyrrolidone, dichloromethane, dimethylformamide, acetonitrile, ethylacetate, tetrahydrofuran, toluene, and CCl_4. During the tests, the aerogels were immersed in oils or organic solvents for 30 minutes, then removed, and the excess oil or solvent was wiped off using a filter paper. Then, the adsorption capacities of BOZ/Si-PHT aerogels were evaluated by

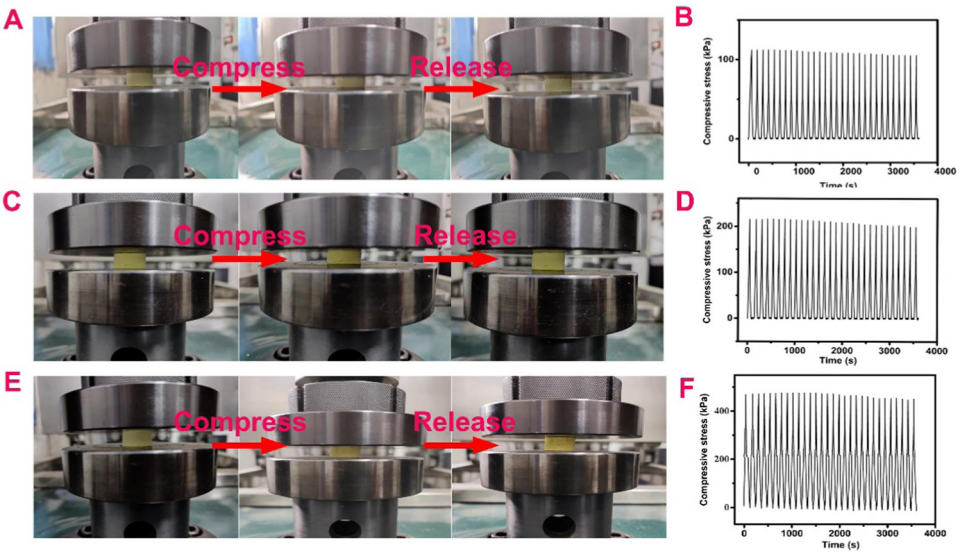

Fig. 3 (A, C and E) Photographs of the compression–recovery process of cylindrical BOZ/Si-PHT-0.1, BOZ/Si-PHT-0.3, and BOZ/Si-PHT-0.5 aerogels, respectively. (B, D and F) 30th Cyclic compress curves of BOZ/Si-PHT-0.1, BOZ/Si-PHT-0.3, and BOZ/Si-PHT-0.5 aerogels, respectively.

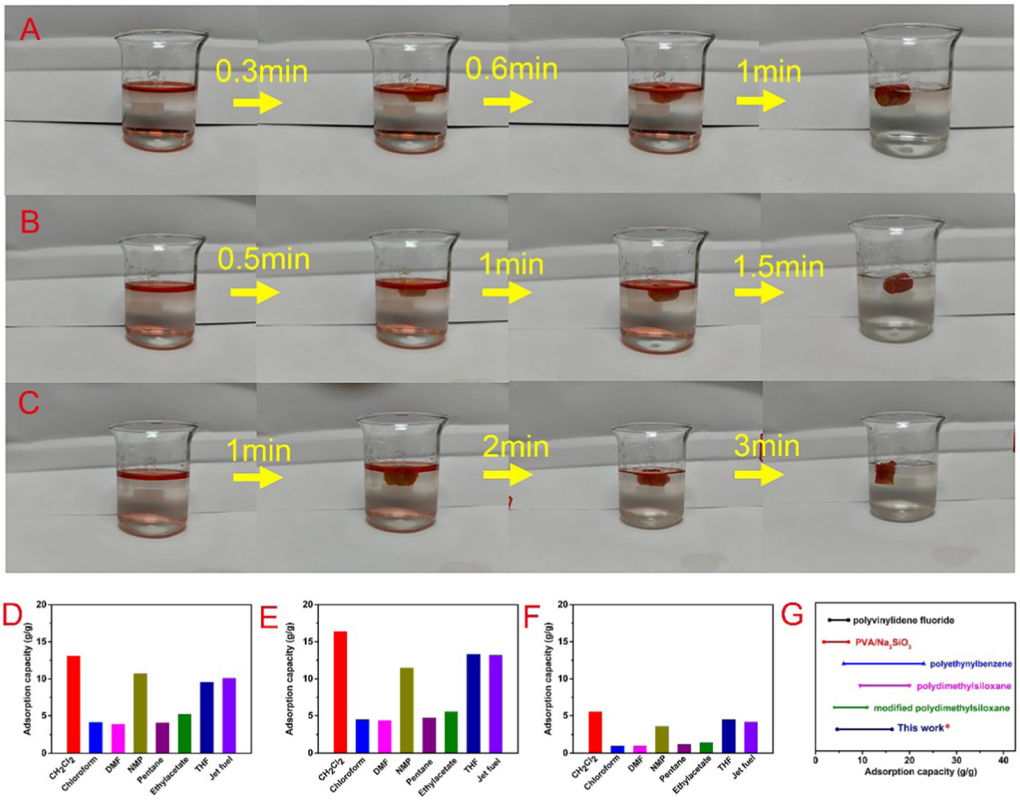

Fig. 4 (A–C) Photographs of the absorption of jet fuel from the surface of water by BOZ/Si-PHT-0.1, BOZ/Si-PHT-0.3, and BOZ/Si-PHT-0.5 aerogels, respectively. (D–F) Maximum absorption capacities of BOZ/Si-PHT-0.1, BOZ/Si-PHT-0.3, and BOZ/Si-PHT-0.5 aerogels for different organic solvents or oils, respectively. (G) Comparison of the adsorption capacity of the BOZ/Si-PHT-0.3 aerogel with other previously published works.

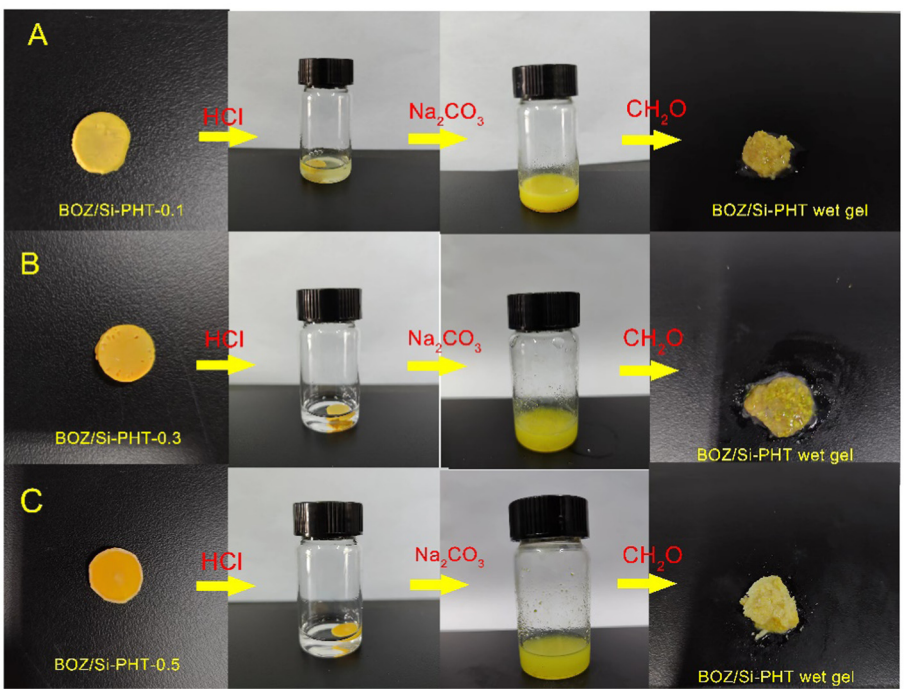

Fig. 5 (A) Cycle process of the BOZ/Si-PHT-0.1 aerogel. (B) Cycle process of the BOZ/Si-PHT-0.3 aerogel. (C) Cycle process of the BOZ/Si-PHT-0.5 aerogel.

the weight differences before and after adsorption. The weight gain range of the BOZ/Si-PHT-0.3 aerogel is 4.6–16.3 times as that of the dry sample. The reason for the difference in absorption capacity may be due to the density and viscosity of liquids. Meanwhile, the BOZ/Si-PHT aerogel exhibits competitive absorption capacity without the complex preparation process, compared with that of other previously reported oil/water separation materials (Fig. 4G) such as the poly(vinylidene fluoride) aerogel (3–7 g g^{-1}),[9] PVA/Na_2SiO_3 porous materials (1.8–7.0 g g^{-1}),[32] conjugated microporous polymers (6–23 g g^{-1}),[33] the polydimethylsiloxane aerogel (9.5–20 g g^{-1}),[34] and sugar-templated polydimethylsiloxane.[35]

The BOZ/Si-PHT aerogel has degradable and recyclable properties, which are an amazing feature compared with other aerogels, especially under environmental pressure from the increased waste of non-degradable aerogels. As shown in Fig. 5(A–C), 0.1 g of the BOZ/Si-PHT aerogel quickly collapses and becomes a yellow cloudy liquid within 1 min, when a 2 mL of 1 N HCl is dropped onto it. The reason is thought to be that, the content of polybenzoxazine is low, the BOZ/Si-PHT network is destroyed by the degradation of polyhexahydrotriazine, and polybenzoxazine is dispersed in the solution in the form of small particles. Then, the saturated Na_2CO_3 solution was added dropwise to the solution until no more bubbles were formed. After this, 0.5 mL of formaldehyde solution (37%) was added into the solution and a yellow BOZ/Si-PHT wet gel was formed again. The adsorption performances of recycled aerogels were tested, and the results were similar to those of the original aerogel. BOZ/Si-PHT aerogels exhibit the recovery and reuse of absorbents, which may mitigate the waste of resources and prohibit secondary pollution, assuring their application under normal circumstances.

4. Conclusion

In this paper, BOZ/Si-PHT IPN aerogels have been facilely prepared using a stepwise curing strategy, followed by low-cost ambient pressure drying. A unique cross-linked interpenetrating network consisting of polyhexahydrotriazine and polybenzoxazine is obtained. The resulting BOZ/Si-PHT aerogels exhibit amazing recycling properties (degrade in 1 N HCl), high hydrophobicity (a contact angle of water of 121.5°), flexible processability (a simple preparation process), good mechanical properties upon compression (a compressive strength of 449.6 kPa, 20.0% of original sizes), and comparably efficient organic solvent/oil absorption and oil water separation (4.3 to 16.3 g g^{-1}). This study is expected to provide new concepts for the synthesis of multifunctional mechanically enhanced and recyclable porous materials promising for practical applications in oil/water separation.

Conflicts of interest

The authors declare that they have no known competing financial interests or personal relationships that could have appeared to influence the work reported in this paper.

Acknowledgements

The research work was supported by the Research Foundation of the Civil Aviation Flight University of China (No. S202110624115), the Sichuan Provincial Science and Technology Department Project (No. MZ2022JB03 and 2023NSFSC0315), and the Civil Aviation Education Talent Project (No. MHJY2022013).

References

1 M. A. Shannon, P. W. Bohn and M. Elimelech, *et al.*, Science and technology for water purification in the coming decades, *Nature*, 2008, **452**(7185), 301–310.
2 W. Zhang, N. Liu and Y. Cao, *et al.*, Superwetting Porous Materials for Wastewater Treatment: from Immiscible Oil/Water Mixture to Emulsion Separation, *Adv. Mater. Interfaces*, 2017, **4**(10), 1600029.
3 J. Chen, W. Zhang and Z. Wan, *et al.*, Oil spills from global tankers: Status review and future governance, *J. Cleaner Prod.*, 2019, **227**, 20–32.
4 V. A. Jernel, How to defend against future oil spills, *Nature*, 2010, **466**(7303), 182–183.
5 T. V. Le, T. Imai and T. Higuchi, *et al.*, Performance of tiny microbubbles enhanced with ''normal cyclone bubbles'' in separation of fine oil-in-water emulsions, *Chem. Eng. Sci.*, 2013, **94**, 1–6.
6 M. Kriipsalu, M. Marques and D. R. Nammari, *et al.*, Biotreatment of oily sludge: The contribution of amendment material to the content of target contaminants, and the biodegradation dynamics, *J. Hazard. Mater.*, 2007, **148**(3), 616–622.
7 Y. Sun, C. Zhu and H. Zheng, *et al.*, Characterization and coagulation behavior of polymeric aluminum ferric silicate for high-concentration oily wastewater treatment, *Chem. Eng. Res. Des.*, 2017, **119**, 23–32.
8 O. M. J. Chapr, D. A. Soares, R. D. C. F. Silva and R. D. Rufino, *et al.*, Formulation and application of a biosurfactant from Bacillus methylotrophicus as collector in the flotation of oily water in industrial environment, *J. Biotechnol.*, 2018, **285**, 15–22.
9 J. Dai, R. Zhang and W. Ge, *et al.*, 3D macroscopic superhydrophobic magnetic porous carbon aerogel converted from biorenewable popcorn for selective oil-water separation, *Mater. Des.*, 2018, **139**, 122–131.
10 J. Jiang, Q. Zhang and X. Zhan, *et al.*, A multifunctional gelatin-based aerogel with superior pollutants adsorption, oil/water separation and photocatalytic properties, *Chem. Eng. J.*, 2019, **358**, 1539–1551.
11 K. Abuhasel, M. Kchaou and M. Alquraish, *et al.*, Oily Wastewater Treatment: Overview of Conventional and Modern Methods, Challenges, and Future Opportunities, *Water*, 2021, **13**(7), 980.
12 S. Sert Çok, F. Ko and N. Gizli, Lightweight and highly hydrophobic silica aerogels dried in ambient pressure for an efficient oil/organic solvent adsorption, *J. Hazard. Mater.*, 2021, **408**, 124858.

13 J. Ren, X. Huang and J. Shi, *et al.*, Transparent, robust, and machinable hybrid silica aerogel with a ''rigid-flexible'' combined structure for thermal insulation, oil/water separation, and self-cleaning, *J. Colloid Interface Sci.*, 2022, **623**, 1101–1110.

14 M. Yang, Z. Chen and T. Liu, *et al.*, Ultralight and robustly compressible silica aerogel enhanced by AC/C sponge with high oil/water separation, *J. Porous Mater.*, 2022, **29**(2), 523–530.

15 J. Lin, G. Li and W. Liu, *et al.*, A review of recent progress on the silica aerogel monoliths: Synthesis, reinforcement, and applications, *J. Mater. Sci.*, 2021, **56**, 10812–10833.

16 Y. Zhang, Q. Shen and X. Li, *et al.*, Facile synthesis of ternary flexible silica aerogels with coarsened skeleton for oil–water separation, *RSC Adv.*, 2020, **10**(69), 42297–42304.

17 C. Yao, X. Dong and G. Gao, *et al.*, Microstructure and Adsorption Properties of MTMS/TEOS Co-precursor Silica Aerogels Dried at Ambient Pressure, *J. Non-Cryst. Solids*, 2021, **562**, 120778.

18 S. Yun, H. Luo and Y. Gao, Superhydrophobic silica aerogel microspheres from methyltrimethoxysilane: rapid synthesis via ambient pressure drying and excellent absorption properties, *RSC Adv.*, 2014, **4**(9), 4535–4542.

19 A. M. Othman, M. M. Ghobashy and N. E. A. Abd El-Sattar, Radiation synthesis of porous calcium silicate aerogel derived from polyacrylamide hydrogel as thermal insulator, *J. Sol-Gel Sci. Technol.*, 2021, **98**(3), 593–604.

20 H. Ramadan, T. Coradin and S. Masse, *et al.*, Synthesis and Characterization of Mesoporous Hybrid Silica-Polyacrylamide Aerogels and Xerogels, *Silicon*, 2011, **3**(2), 63–75.

21 S. Rezaei, A. M. Zolali and A. Jalali, *et al.*, Novel and simple design of nanostructured, super-insulative and flexible hybrid silica aerogel with a new macromolecular polyether-based precursor, *J. Colloid Interface Sci.*, 2020, **561**, 890–901.

22 Z. Kantor, T. Wu and Z. Zeng, *et al.*, Heterogeneous silica-polyimide aerogel-in-aerogel nanocomposites, *Chem. Eng. J.*, 2022, **443**, 136401.

23 S. Salimian, W. J. Malfait and A. Zadhoush, *et al.*, Fabrication and evaluation of silica aerogel-epoxy nanocomposites: Fracture and toughening mechanisms, *Theor. Appl. Fract. Mech.*, 2018, **97**, 156–164.

24 A. Katti, N. Shimpi and S. Roy, *et al.*, Chemical, Physical, and Mechanical Characterization of Isocyanate Cross-linked Amine-Modified Silica Aerogels, *Chem. Mater.*, 2006, **18**(2), 285–296.

25 Z. Kantor, T. Wu and Z. Zeng, *et al.*, Heterogeneous silica-polyimide aerogel-in-aerogel nanocomposites, *Chem. Eng. J.*, 2022, **443**, 136401.

26 M. M. Umair, Y. Zhang and K. Iqbal, *et al.*, Novel strategies and supporting materials applied to shape-stabilize organic phase change materials for thermal energy storage–A review, *Appl. Energy*, 2019, **235**, 846–873.

27 M. C. Prete and C. R. T. Tarley, Bisphenol A adsorption in aqueous medium by investigating organic and inorganic components of hybrid polymer (polyvinylpyridine/SiO_2/APTMS), *Chem. Eng. J.*, 2019, **367**, 102–114.

28 Y. Xu, Z. Li and X. Sun, *et al.*, Enhanced toughness and degradable ability of polybenzoxazines/polyhexahydrotriazines interpenetrating polymer networks by sequential cure method, *Mater. Today Chem.*, 2022, **24**, 100937.

29 I. Helmers, M. Niehues and K. K. Kartha, *et al.*, Synergistic repulsive interactions trigger pathway complexity, *Chem. Commun.*, 2020, **56**(63), 8944–8947.

30 G. Liu, J. Li and X. Li, *et al.*, Preparation and properties of novel superhydrophobic cellulose nanofiber aerogels, *J. Nanomater.*, 2021, **2021**, 1–8.

31 Y. Lei, W. Shi and S. Ding, *et al.*, In-situ benzoxazine-isocyanide chemistry (BIC)/sol-gel preparation and Pb(II) electrochemical probing investigation of modified polyamide/silica composite, *Colloids Surf., A*, 2022, **632**, 127798.

32 Q. Wang, Q. Li and M. Yasir Akram, *et al.*, Decomposable Polyvinyl Alcohol-Based Super-Hydrophobic Three-Dimensional Porous Material for Effective Water/Oil Separation, *Langmuir*, 2018, **34**(51), 15700–15707.

33 A. Li, H.-X. Sun and D.-Z. Tan, *et al.*, Superhydrophobic conjugated microporous polymers for separation and adsorption, *Energy Environ. Sci.*, 2011, **4**(6), 2062–2065.

34 K. Wang, X. Liu and Y. Tan, *et al.*, Two-dimensional membrane and three-dimensional bulk aerogel materials via top-down wood nanotechnology for multibehavioral and reusable oil/water separation, *Chem. Eng. J.*, 2019, **371**, 769–780.

35 S.-J. Choi, T.-H. Kwon and H. Im, *et al.*, A Polydimethylsiloxane (PDMS) Sponge for the Selective Absorption of Oil from Water, *ACS Appl. Mater. Interfaces*, 2011, **3**(12), 4552–4556.